

## Supplementary information

# Switchable single fluorescent polymeric nanoparticles for stable white-light generation

Hong Wang,<sup>1,a</sup> Peisheng Zhang,<sup>1,a</sup> Baiju P. Krishnan,<sup>b</sup> Maolin Yu,<sup>a</sup> Jie Liu,<sup>a</sup> Mingju Xue,<sup>a</sup> Shu Chen,<sup>a</sup> Rongjin Zeng,<sup>a</sup> Jiaxi Cui<sup>\*b,c</sup> and Jian Chen<sup>\*a</sup>

<sup>a</sup>Key Laboratory of Theoretical Organic Chemistry and Function Molecule, Ministry of Education, Hunan Provincial Key Laboratory of Controllable Preparation and Functional Application of Fine Polymers, Hunan Province College Key Laboratory of QSAR/QSPR, School of Chemistry and Chemical Hunan University of Science and Technology Xiangtan 411201, P. R. China.

<sup>b</sup>INM-Leibniz Institute for New Materials Campus D2 2, 66123 Saarbrücken (Germany)

<sup>c</sup>Institute of Fundamental and Frontier Sciences, University of Electronic Science and Technology of China, Chengdu, Sichuan, 610054, China

\* Corresponding authors: [cj0066@gmail.com](mailto:cj0066@gmail.com) (J. Chen); [jiaxi.cui@leibniz-inm.de](mailto:jiaxi.cui@leibniz-inm.de) (J. Cui)

<sup>1</sup>These authors contributed equally.

## Experimental section

### Materials

The surfactant cetyltrimethyl ammonium chloride (CTAC, 99%), n-hexadecane (HD, 99%), divinylbenzene (DVB, 99%) and styrene (St, 99%) are used as received from Sigma-Aldrich. Azobisisobutyronitrile (AIBN, 99.99%, Aldrich) was recrystallized from ethanol and dried under vacuum. Other reagents were analytical reagents and used without further purification. The double-distilled water used in this work was further purified with a Milli-Q system. All other reagents were analytical reagents and used without further purification. 4-phenylenebis((4-(diphenylamino)phenyl)methanone) (*p*-DTPACO) and spiropyran-linked methacrylate (SPMA) are synthesized according to the methods in our previous reports<sup>[1-2]</sup>.

### Characterization

<sup>1</sup>H NMR spectra were recorded on a Bruker Avance 500 MHz NMR spectrometer. The nanoparticle diameters were determined by a Malvern Nano-ZS90 instrument and their

morphology was observed with a JEM-2100F transmission electron microscope (TEM, JEOL USA, Inc.). UV-Vis spectra were recorded on a Shimadzu. Fluorescence spectra and fluorescence lifetime ( $\tau$ ) measurements were carried out with a time-correlated single photon counting (TCSPC) nanosecond fluorescence spectrometer (Edinburgh FLS920) at ambient temperature (298 K).

### **Synthesis of FPNs**

A mixture containing the monomer (St, 0.49 g); crosslinker (DVB, 0.01 g), hydrophobic dyes (*p*-DTPACO, 6 mg), SP-based methacrylate monomer (SPMA, 20 mg), polymerization initiator (AIBN, 0.025 g), and hydrophobe (HD, 0.075 g) was added to 10 mL water solution with emulsifier (CTAC, 0.1 g) and stirred (1000 r/min) for 10 min, then, the mixture was ultrasonicated for 15 min (JY92-IIN) to obtain a stable miniemulsion. The mixture was cooled in an ice-bath during ultrasonication to avoid overheating. The resulting miniemulsion was put into a 50 mL flask equipped with a condenser, which was immersed in an oil bath with a thermostat. The miniemulsion was polymerized at 75 °C for 4 h. After the polymerization, the as-prepared nanoparticle dispersions were dialyzed three times to remove uncombined monomers. Finally, a stable FPNs dispersion was obtained. The stable FPNs containing different amount of *p*-DTPACO and SPMA was obtained. The detail experimental parameters for this polymerization are shown in Table S2.

### **Swelling and deswelling experiment**

The solution of FPN-3 (0.075 mL) added into 2.925 mL of water and then the different volume of DCM (Table S4) was added into above solution. The mixture solution was stirred acutely for 2 h. The optical spectrum of the above solution was obtained. In deswelling experiment, DCM was removed by a rotary evaporator at 20 °C for 2 h.

### **Estimation of the photochemical conversion yield from SP to MC**

The photochemical conversion yield from SP to MC can be obtained by UV/Vis spectroscopy. According to the literature report, generally the molar absorption coefficient, or extinction coefficient ( $\epsilon_A$ ) of MC in polar solvents at  $\lambda_{\max}$  (566 nm) is 35,000 mol<sup>-1</sup>. L. cm<sup>-1</sup> (J. B. Flannery, Jr. *J. Am. Chem. Soc.*, 1968, 90, 5660-5671.), we used this value as the extinction coefficient of MC in nanoparticles because the polymer styrene (PS) for the dyes is the polar

matrix. Thus, we can estimate the photochemical conversion yield ( $\Phi_c$ ) from SP to MC via the equation [Eq. S1] below:

$$\Phi_c = \frac{A}{\varepsilon_A LC_0} \quad [\text{Eq. S1}]$$

Where  $A$  is the absorbance for MC at 566 nm upon UV irradiation,  $\varepsilon_A$  is the molar absorption coefficient ( $\varepsilon_A$ ) of MC at the  $\lambda_{\text{max}}$  (566nm),  $L$  is the path length of the sample (1 cm for the present case), and  $C_0$  is the actual mole concentration of spiropyran in NP dispersions. The obtained photochemical conversion yields for some samples are listed in Table S2.

#### **Determination of Quantum Yield (QY).**

RHB in ethanol (QY is 0.65) was used as the reference standard. The QY of *p*-DTPACO were calculated:

$$\Phi_p = \Phi_R \times \frac{I_p}{I_R} \times \frac{A_R}{A_p} \times \frac{\eta_p^2}{\eta_R^2} \quad [\text{Eq. S2}]$$

where  $\Phi_R$  is QY of RHB in ethanol,  $I$  is the integrated emission intensity,  $A$  represents absorbance, and  $\eta$  is the solvent refractive index, respectively. For achieving the precious results, *p*-DTPACO and referenced samples adjusted the absorption below 0.10 (fluorescence cuvette). The PL spectra were recorded with the fluorimeter. Similarly, the  $\Phi_p$  of *p*-DTPACO in nanoparticle system (sample FPN-1) upon Vis/UV irradiation was calculated as 16.8 % (Vis) and 2.9 % (UV).

#### **Calculation of the Förster radii ( $R_0$ )**

The Förster's distance or critical distance  $R_0$  is the characteristic distance between the donor and the acceptor, at which the efficiency of energy transfer is 50%. The magnitude of  $R_0$  is dependent on the spectral properties of the donor and acceptor molecules. If the wavelength  $\lambda$  is expressed in nanometers, then  $J(\lambda)$  is in units of  $\text{M}^{-1} \text{cm}^{-1} \text{nm}^4$  and the Förster distance,  $R_0$  in angstroms ( $\text{\AA}$ ), is expressed as follows <sup>[4,5]</sup> [Eq. S3]:

$$R_0 = 0.2108 \times [\kappa^2 \times \Phi_D \times n^4 \times J(\lambda)]^{1/6} \quad [\text{Eq. S3}]$$

$K^2$  is the orientation factor for the emission and absorption dipoles and its value depends on their relative orientation,  $n$  is the refractive index of the medium and  $\Phi_D$  is the quantum yield of the donor.  $J(\lambda)$  is the overlap integral of the fluorescence emission spectrum of the donor and the absorption spectrum of the acceptor (Figure S7) [Eq. S4].

$$J(\lambda) = \int_0^{\infty} F_D(\lambda) \times \varepsilon_A(\lambda) \times \lambda^4 \times d\lambda \quad [\text{Eq. S4}]$$

where  $F_D(\lambda)$  is the fluorescence intensity of the donor in the absence of acceptor,  $\varepsilon_A(\lambda)$  is molar extinction coefficient of the acceptor SPMA (35,000 mol<sup>-1</sup>.L.cm<sup>-1</sup> for polar solution was used for the calculation),  $\lambda$  is wavelength. In current experimental conditions, the Förster distances ( $R_0$ ) have been calculated assuming random orientation of the donor and acceptor molecules taking  $K^2 = 2/3$ ,  $n = 1.59$  (PS). For *p*-DTPACO (donor) and SPMA (acceptor) in current experimental situation, we calculated  $R_0 = 42 \text{ \AA}$ . Energy transfer will be effective for  $d \leq 63 \text{ \AA}$  (upper limit:  $R_0 + 50\% R_0$ ).<sup>[6]</sup>

### **Calculation of experimental energy transfer efficiency and estimation of donor-acceptor distance**

According to the Förster non-radiative energy transfer theory, the energy transfer efficiency  $E$  depends not only on the distance ( $r$ ) between the donor (*p*-DTPACO) and the acceptor (SPMA), but also on the critical energy transfer distance ( $R_0$ ) expressed by the following equation [Eq. S5]:

$$E = \frac{R_0^6}{R_0^6 + r^6} \quad [\text{Eq. S5}]$$

The FRET efficiency can be measured experimentally and is commonly defined as

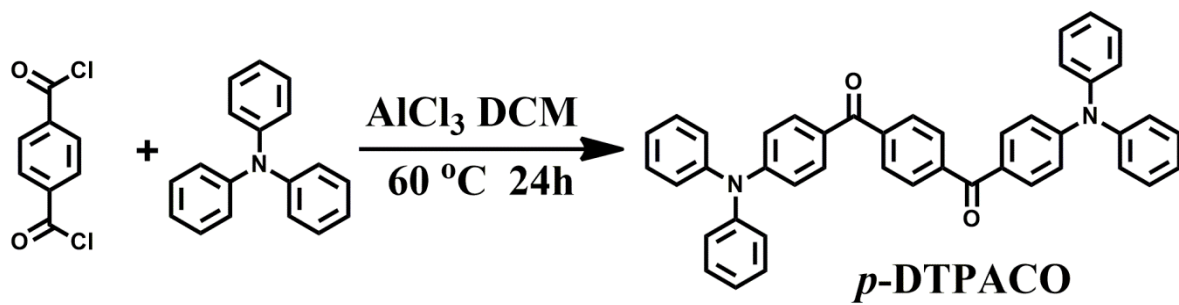
$$E = 1 - \frac{F}{F_0} \quad [\text{Eq. S6}]$$

where  $F$  and  $F_0$  is the fluorescence intensity of the donor in the presence or absence of the acceptor, respectively.<sup>[4,5]</sup>

By combining Equation S5 and S6, we can obtain an expression [Eq. S7] for the donor-acceptor separation distance for each sample which can be experimentally determined from fluorescence data.

$$r = R_0 \left[ \frac{(1-E)}{E} \right]^{1/6} \quad [\text{Eq. S7}]$$

The calculated data are listed in Table S2.



**Scheme S1.** Synthesis of 4-phenylenebis((4-(diphenylamino)phenyl)methanone) (*p*-DTPACO).

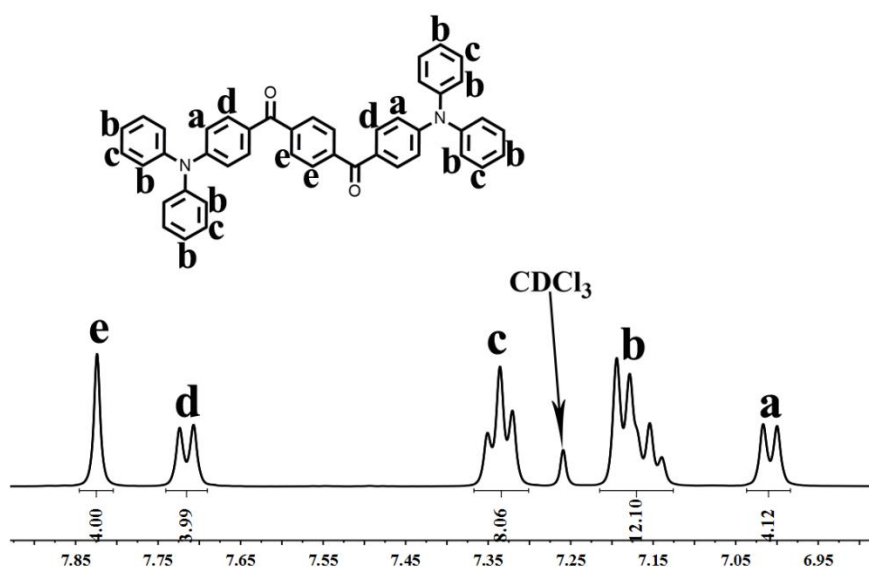


**Figure S1.** <sup>1</sup>H NMR spectra of the *p*-DTPACO in CDCl<sub>3</sub>.

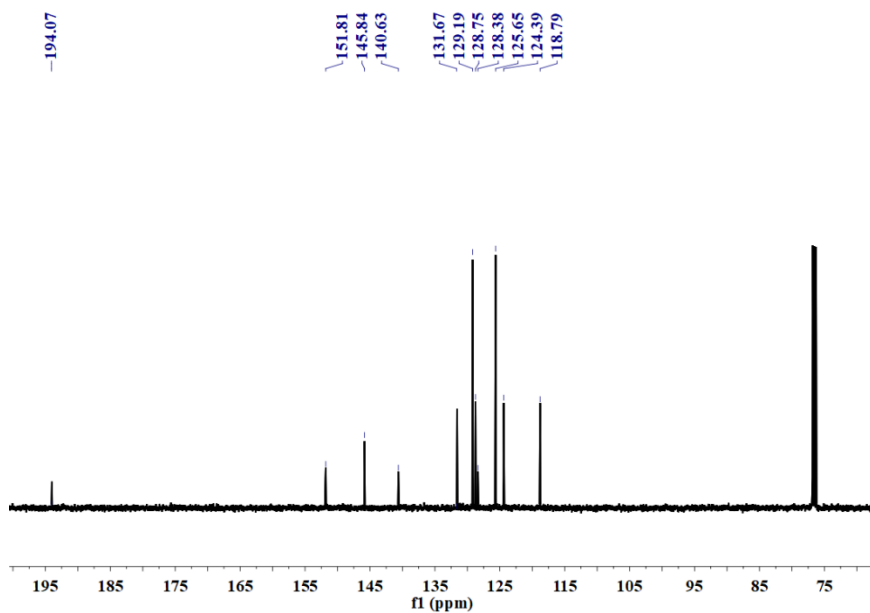


**Figure S2.**  $^{13}\text{C}$  NMR spectra of the *p*-DTPACO in  $\text{CDCl}_3$ .

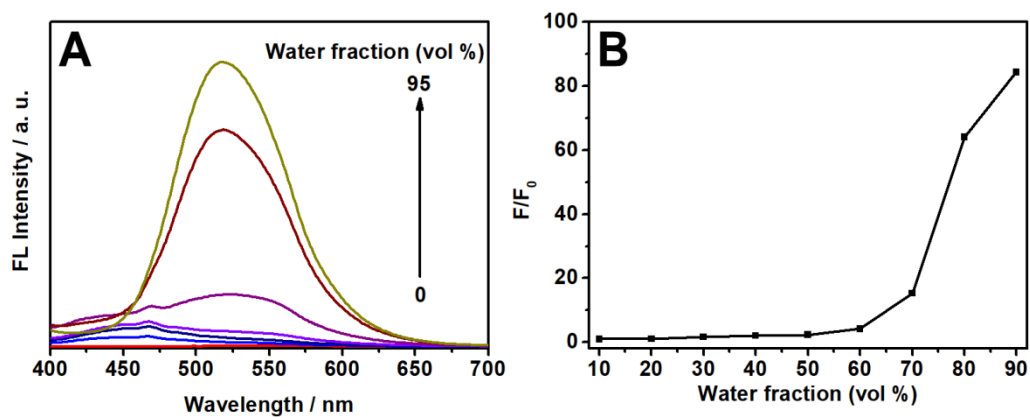


**Figure S3.** (A) The fluorescence emission spectra of *p*-DTPACO in water/THF mixtures with varied water content. (B) Plot of  $F/F_0$  at 520 nm versus water content (%), where  $F_0$  is the fluorescence intensity in pure THF solution.  $\lambda_{\text{ex}} = 420$  nm.

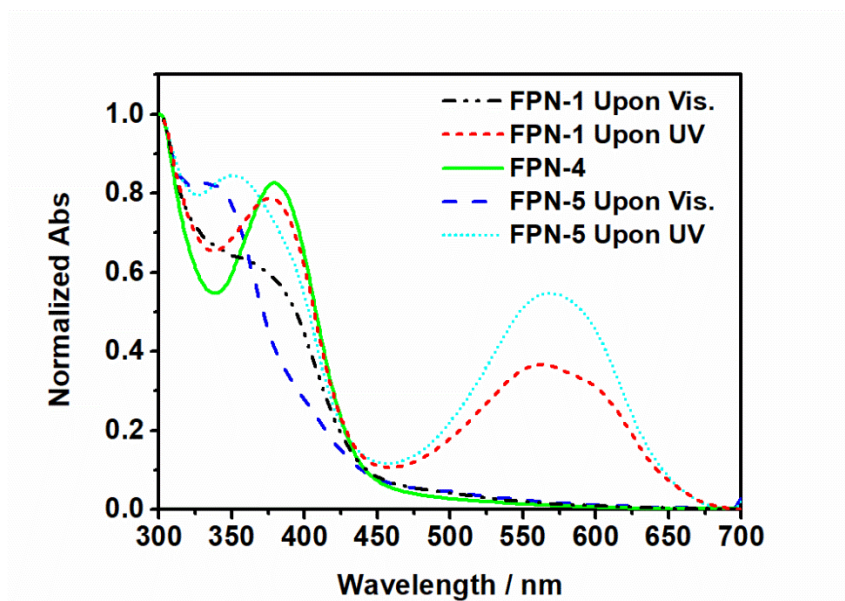


**Figure S4.** Normalized absorption spectra of FPN-1, FPN-4 and FPN-5 upon UV (365 nm, 2.8 mW/cm<sup>2</sup>) or visible light (525, 1.34 mW/cm<sup>2</sup>).

**Table S1.** Composition and characteristics of polymeric nanoparticles

No. <sup>a</sup>	<i>p</i> -DTPACO <sup>b</sup> (mg)	Diameter <sup>c</sup> (nm)	PDI <sup>d</sup>
NP-1	1	65	0.232
NP-2	6	60	0.205
NP-3	10	67	0.219
NP-4	15	62	0.215

<sup>a</sup>The St/ DVB/HD/CTAC/AIBN feed is 0.49/0.01/0.075/0.1/0.025 g, respectively;

<sup>b</sup>Weight of *p*-DTPACO (donor) in dispersion;

<sup>c</sup>Hydrodynamic diameter of nanoparticles samples obtained from DLS;

<sup>d</sup>PDI of nanoparticles samples obtained from DLS.

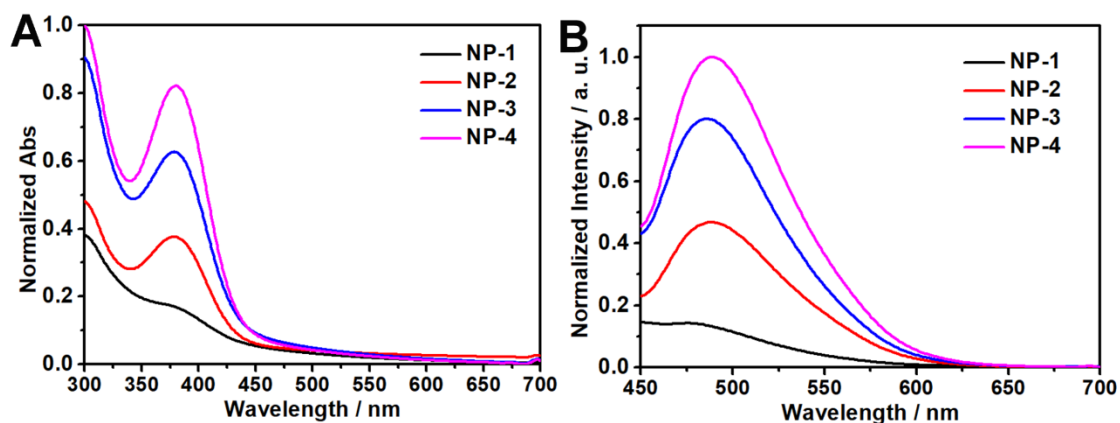


**Figure. S5.** Normalized absorption (A) and fluorescence (B) spectra of various *p*-DTPACO in nanoparticles (solid content: 0.138 wt%,  $\lambda_{\text{ex}} = 420$  nm).

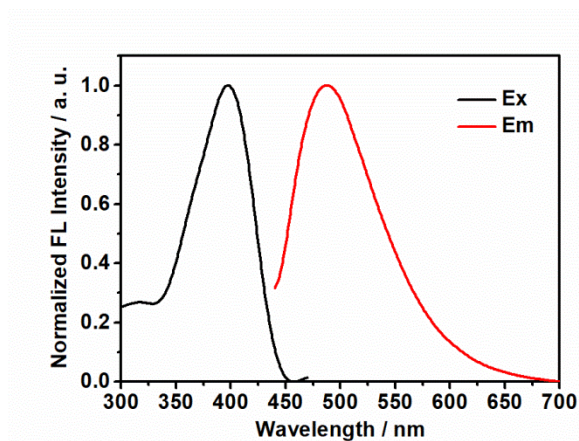


**Figure S6.** Excitation and fluorescence emission spectra of FPN-4.



**TableS2.** Composition and characteristics of polymeric nanoparticles

No. <sup>a</sup>	<i>p</i> -DTPACO <sup>b</sup> (mg)	SPMA <sup>c</sup> (mg)	Diameter <sup>d</sup> (nm)	PDI <sup>e</sup>	<i>E</i> <sup>f</sup>	$\Phi_c$ <sup>g</sup>	<i>r</i> <sup>h</sup> (nm)
FPN-1	6	20	60	0.205	93.8%	0.151	2.7
FPN-2	6	7	63	0.209	81.7%	0.130	3.3
FPN-3	6	4.6	58	0.192	68.2%	0.139	3.7
FPN-4	6	0	60	0.197	--	--	--
FPN-5	0	20	62	0.215	--	0.148	--

<sup>a</sup>The St/DVB/HD/CTAC/AIBN feed is 0.49/0.01/0.075/0.1/0.025 g, respectively;

<sup>b</sup>Weight of *p*-DTPACO (donor) in dispersion;

<sup>c</sup>Weight of SPMA (acceptor) in dispersion;

<sup>d</sup>Hydrodynamic diameter of nanoparticles samples obtained from DLS;

<sup>e</sup>PDI of nanoparticles samples obtained from DLS;

<sup>f</sup>The energy transfer efficiency (*E*) determined by the equation:  $E=[1-F/F_0]$ , where F is the maximum fluorescence intensity of the donor at 494 nm under visible or UV light irradiation. F<sub>0</sub> is maximum fluorescence intensity of FPN-4 at 494 nm.

<sup>g</sup>The photochemical conversion yield from SP to MC obtained by UV/Vis spectroscopy ( $\Phi_c=0.265$ , acetonitrile).

<sup>h</sup>The average separation distance (*r*) of the donor and the acceptor moieties was calculated by [Eq. S7].

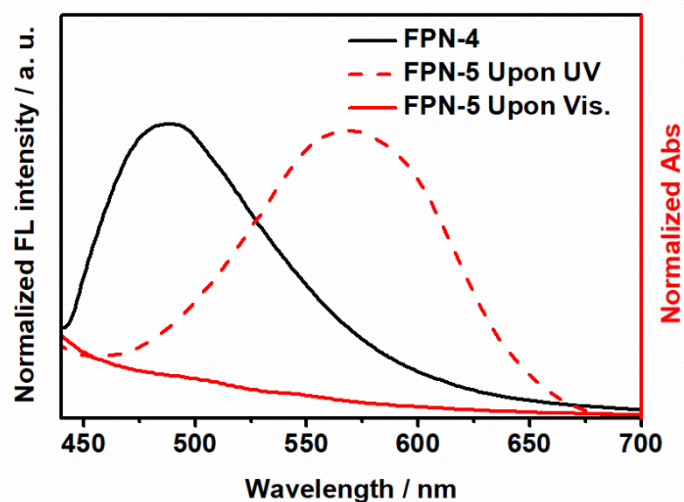


**Figure S7.** Absorption spectra of the SP state (red solid curve) and MC state (red dashed curve) of spiropyran units in polymer nanoparticles sample (FPN-5) (solid content: 0.138 wt%) and fluorescence emission spectra of FPN-4 (solid content: 0.138 wt%,  $\lambda_{\text{ex}} = 420$  nm) contained only *p*-DTPACO (black solid curve).

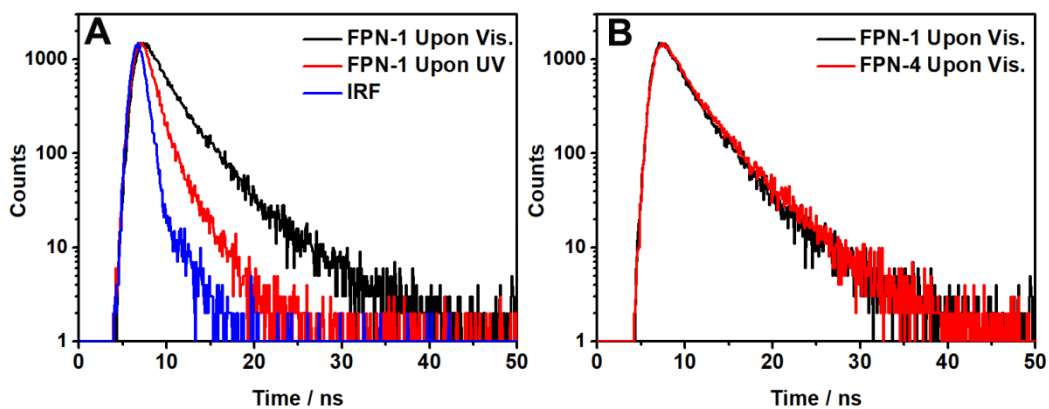


**Figure S8.** (A) Fluorescence decay curves of the nanoparticles sample FPN-1 (solid content: 0.138 wt%) upon Vis/UV light irradiation ( $\lambda_{\text{ex}} = 420$  nm,  $\lambda_{\text{em}} = 494$  nm). (B) Fluorescence decay curves of the nanoparticles sample FPN-1 and FPN-4 (solid content: 0.138 wt%) upon Vis light irradiation ( $\lambda_{\text{ex}} = 420$  nm,  $\lambda_{\text{em}} = 494$  nm).

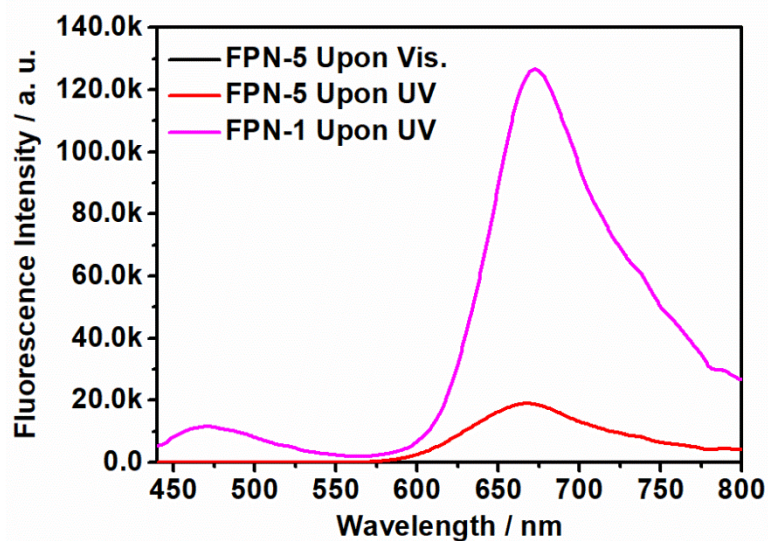


**Figure S9.** Fluorescence emission spectra of FPN-5 modulated by visible light (525 nm, 1.34 mW/cm<sup>2</sup>) or UV (365 nm, 2.8 mW/cm<sup>2</sup>) irradiation and FPN-1 modulated by UV (365 nm, 2.8 mW/cm<sup>2</sup>),  $\lambda_{\text{ex}} = 420$  nm.

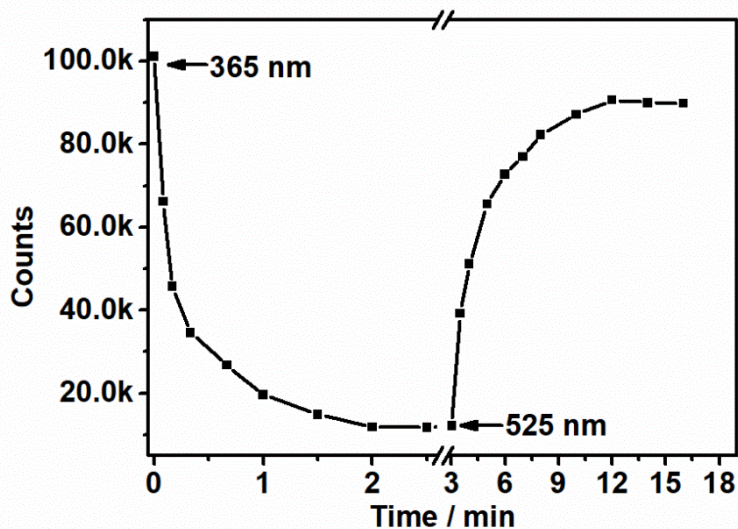


**Figure S10.** Fluorescence response of FPN-1 (solid content: 0.138 wt%) under UV (365 nm, 2.8 mW/cm<sup>2</sup>) and visible light (525 nm, 1.34 mW/cm<sup>2</sup>) irradiation at 494 nm,  $\lambda_{\text{ex}} = 420$  nm.

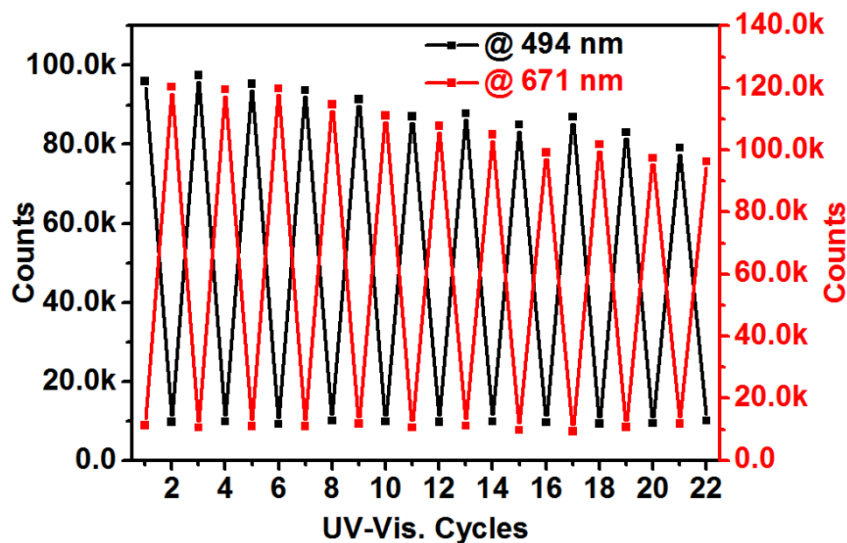


**Figure S11.** Photoinduced switching cycles of FPN-1 (solid content: 0.138 wt%) under alternative illumination of UV for 3 min and visible light for 13 min ( $\lambda_{\text{ex}} = 420$  nm,  $\lambda_{\text{em}} = 494$  nm and 671 nm).

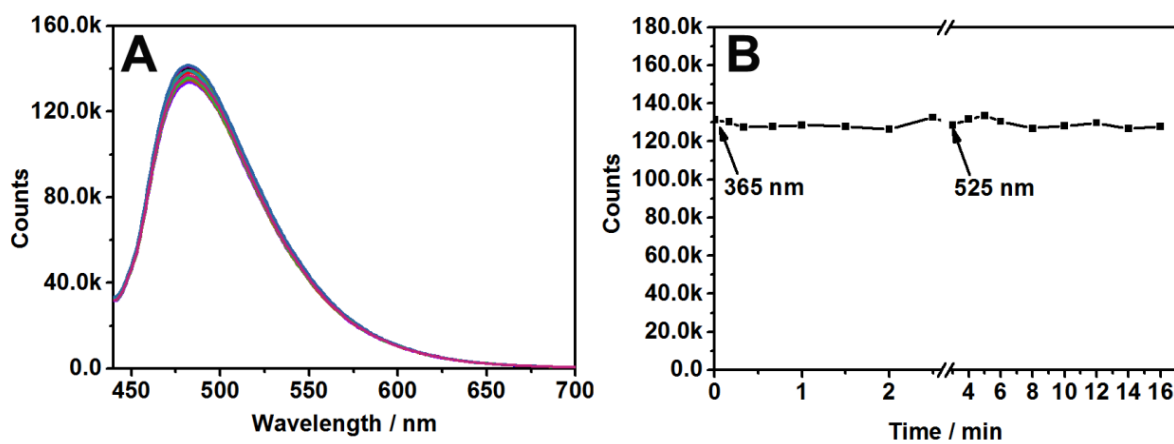


**Figure S12.** Fluorescent emission spectra (A) and intensity changes at 494 nm for the FPN-4 containing only *p*-DTPACO (solid content: 0.138 wt%) via irradiating with UV (365 nm, 2.8 mW/cm<sup>2</sup>) and visible light (525 nm, 1.34 mW/cm<sup>2</sup>),  $\lambda_{\text{ex}} = 420$  nm.

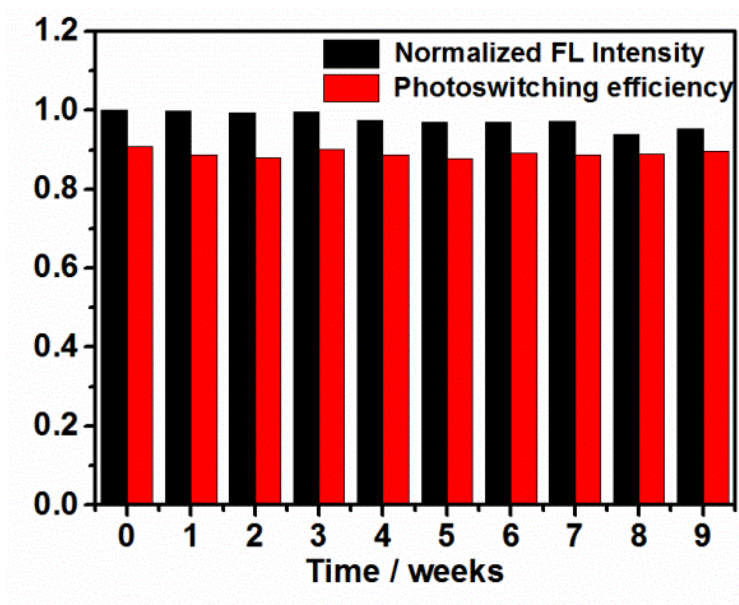


**Figure S13.** Long-term fluorescence stability of FPN-1 (solid content: 0.138 wt%,  $\lambda_{ex}$ =420 nm,  $\lambda_{em}$  = 494 nm).

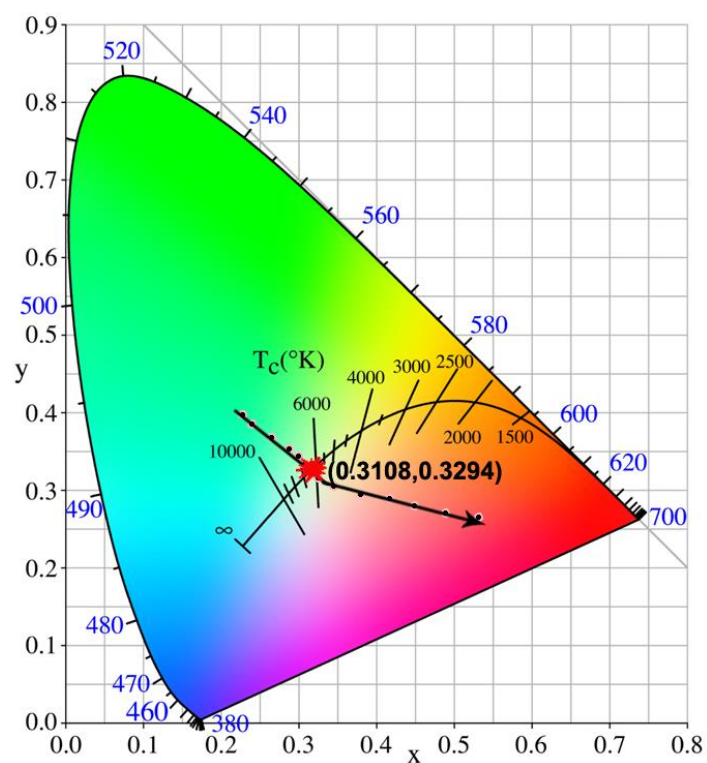


**Figure S14.** CIE 1931 chromaticity coordinates of mixing FPN-1 under the different time of UV irradiation.

**Table S3.** CIE and CCT Values for White-Light-Emitting Systems

System	CIE	CCT (K)
FPN-1--white	0.3108, 0.3294	6605 ±200
FPN-3--white	0.3045, 0.3164	7121 ±200

McCamy's formula Correlated color temperature as an explicit function of chromaticity coordinates. CCT is expressed as follows [Equation S1 and S2]:<sup>[7]</sup>

$$\text{CCT} = -449n^3 + 3525n^2 - 6823.3n + 5520.33 \quad [\text{Equation S1}]$$

$$n = (x - 0.3320) / (y - 0.1858) \quad [\text{Equation S2}]$$

**Table S4.** Summary of some data for FPN-3 under various concentrations of DCM.

No. <sup>a</sup>	DCM <sup>b</sup> ( $\mu$ L)	Diameter <sup>c</sup> (nm)	PDI <sup>d</sup>	<i>E</i> <sup>e</sup>
FPN-D1	0	58	0.192	68.2%
FPN-D2	10	60	0.203	69.4%
FPN-D3	20	69	0.210	76.5%
FPN-D4	30	87	0.317	82.1%
FPN-D5	40	89	0.280	79.7%

<sup>a</sup>The solid content is 0.138 wt% (solution volume: 3 mL);

<sup>b</sup>Volume of DCM in solution;

<sup>c</sup>Hydrodynamic diameter of nanoparticles samples obtained from DLS;

<sup>d</sup>PDI of nanoparticles samples obtained from DLS.

<sup>e</sup>The energy transfer efficiency (*E*) determined by the equation:  $E = [1 - F/F_0]$ , where  $F_0$  and  $F$  is the maximum fluorescence intensity of the donor at 494 nm under visible or UV light irradiation.

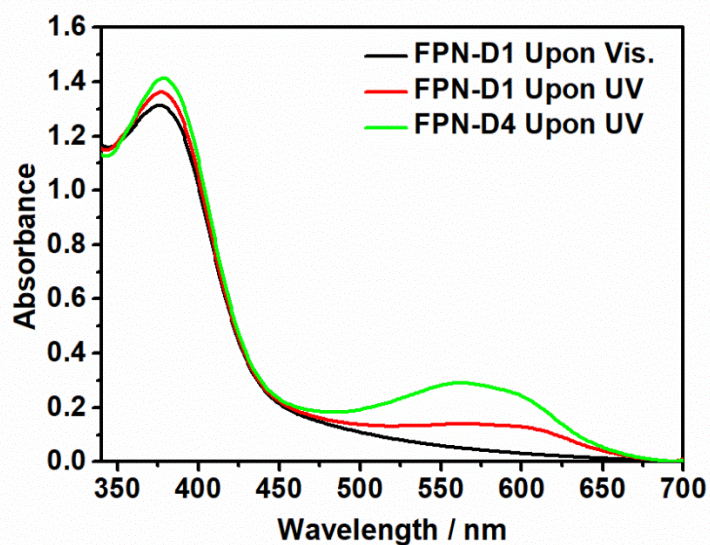


**Figure S15.** Absorption spectra of FPN-3 (solid content: 0.138 wt%) without or with DCM swelling (Table S4) after Vis. or UV irradiation.

Note:  $\Phi_{c(\text{swelling})}=0.239$ ,  $\Phi_{c(\text{deswelling})}=0.139$ .

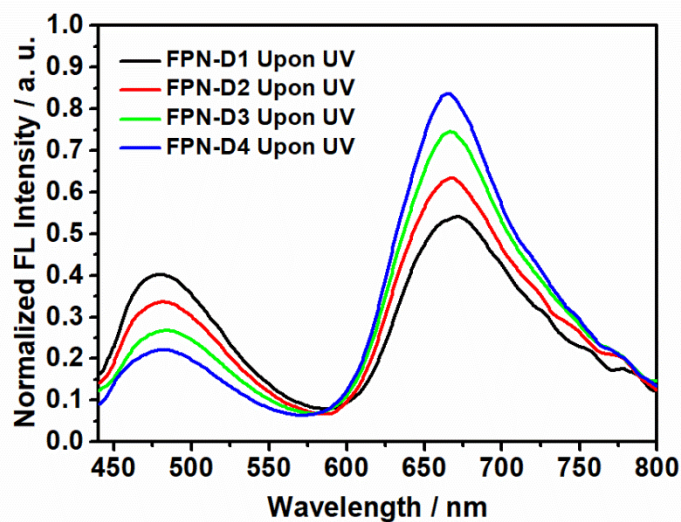


**Figure S16.** Fluorescence spectrum of FPN-3 without or with swelling of various concentrations of DCM (Table S4) after UV irradiation,  $\lambda_{\text{ex}} = 420$  nm.

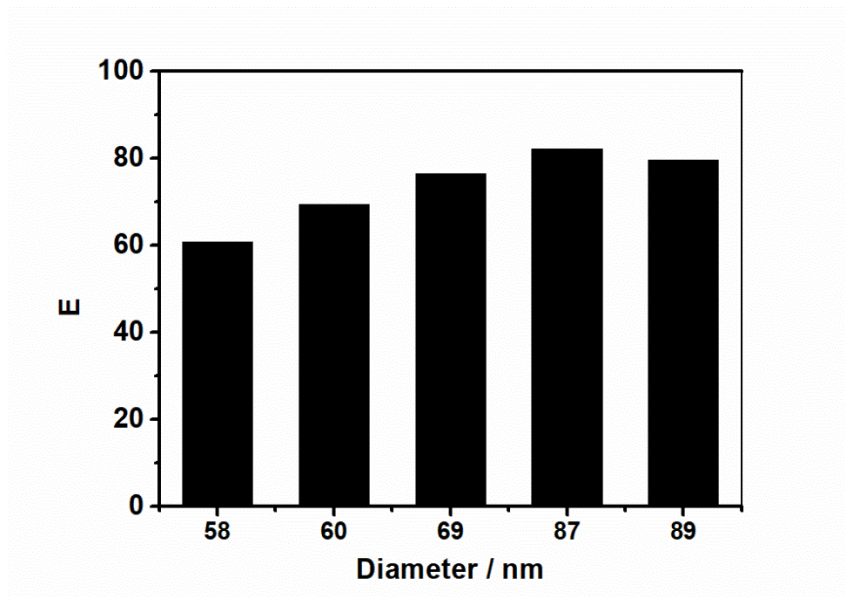


**Figure S17.** Relationship between energy transfer efficiency ( $E$ ) with diameter (FPN-3).

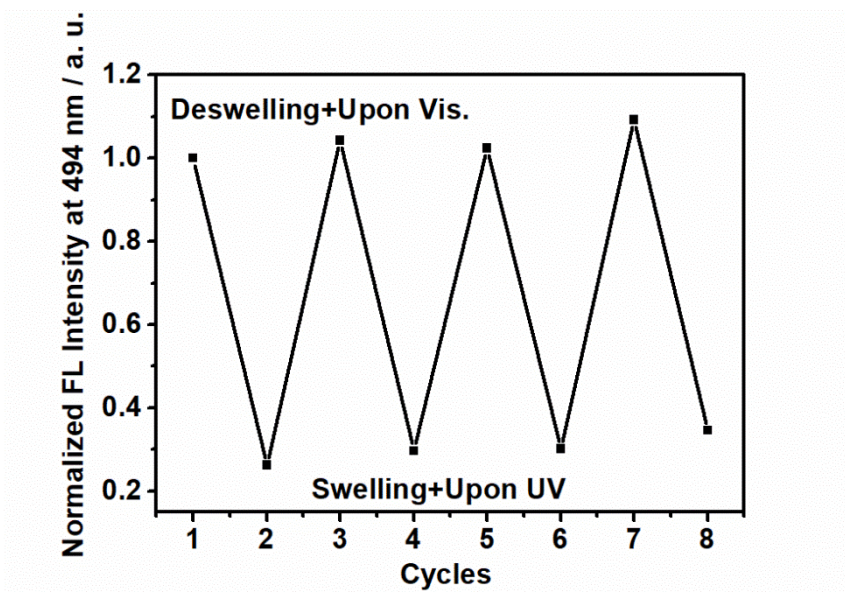


**Figure S18.** Fluorescence switching of FPN-3 (solid content: 0.138 wt%) under UV/Vis. irradiation together with swelling/deswelling of DCM (30  $\mu$ L),  $\lambda_{\text{ex}} = 420$  nm.



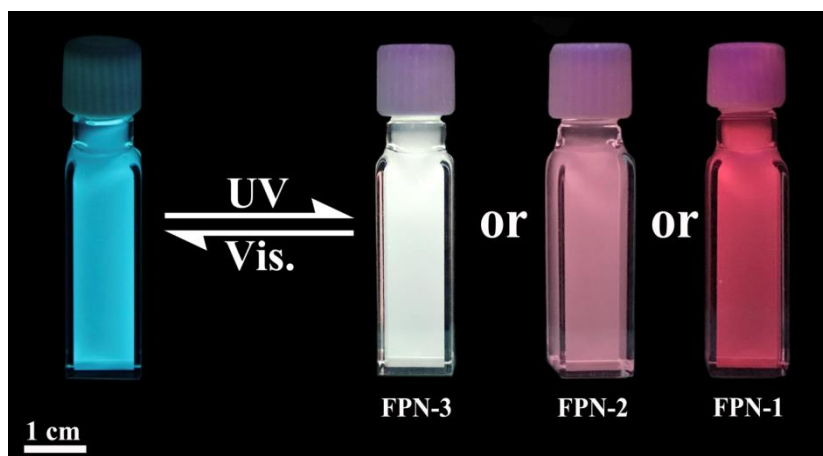


**Figure S19.** Reversible fluorescence picture of SFPN (solid content: 0.138 wt%) in cuvettes under a UV light (365 nm) excitation by UV irradiation for 2 min.

## References

- [1] W. Zhong, X. Zeng, J. Chen, Y. Hong, L. Xiao, P. Zhang, *Polym. Chem.* **2017**, *8* (33), 4849-4855.
- [2] J. Chen, W. Zhong, Y. Tang, Z. Wu, Y. Li, P. Yi, J. Jiang, *Macromolecules* **2015**, *48* (11), 3500-3508.
- [3] S. Yang, C. Zhu, J. Song, H. Li, D. Du, Y. Lin, *ACS Appl. Mater. Interfaces* **2017**, *9*, 7399-7405.
- [4] J. R. Lakowicz, *Principles of Fluorescence Spectroscopy*; Plenum: New York, **1999**.
- [5] B. Valeur in *Molecular Fluorescence: principles and applications*, Wiley-VCH, Weinheim, New York, **2002**.
- [6] K. E. Sapsford, L. Berti, and I. L. Medintz, *Angew. Chem. Int. Ed.*, **2006**, *45*, 4562-4588.
- [7] C. S. McCamy, Correlated color temperature as an explicit function of chromaticity coordinates. *Color Research&Application*, **1992**, *17*(2):142.